PHYSICS OF FLUIDS **27**, 082003 (2015)

Dynamics of oppositely charged emulsion droplets

Zhou Liu,[1,2] Hans M. Wyss,[3] Alberto Fernandez-Nieves,[4] and Ho Cheung Shum[1,2,a)]
[1]*Department of Mechanical Engineering, The University of Hong Kong, Hong Kong*
[2]*HKU-Shenzhen Institute of Research and Innovation (HKU-SIRI), Shenzhen, Guangdong, China*
[3]*Institute for Complex Molecular Systems (ICMS) and Department of Mechanical Engineering, Eindhoven University of Technology, 5612 AZ Eindhoven, The Netherlands*
[4]*School of Physics, Georgia Institute of Technology, Atlanta, Georgia 30332, USA*

(Received 23 February 2015; accepted 29 June 2015; published online 28 August 2015)

We study the dynamics of two pinned droplets under the influence of an applied electric stress. We find that at a sufficiently strong field, this stress is sufficient to induce contact of the droplets. Interestingly, upon such contact, the dynamic behavior sensitively depends on the separation distance between the droplets. Besides the classical "coalescence" regime, we identify two other dynamic regimes: "fuse-and-split" and "periodic non-coalescence." In the "fuse-and-split" regime, the droplets first fuse to form a jet, which subsequently breaks up into two droplets. In the "periodic non-coalescence" regime, the droplets contact and bounce away periodically without coalescence. Further analysis indicates that while the electric stress stretches the droplets into shapes that depend on the initial droplet separation, the surface tension stress dominates over the electric stress as soon as the droplets touch. We show that the shapes of the contacting droplets determine their subsequent dynamics. Our work provides a rationale for understanding the interplay between surface tension and electric stresses that govern the behavior of charged droplets and could inspire new methods for characterizing emulsion stability and surfactant performance. [http://dx.doi.org/10.1063/1.4928854]

I. INTRODUCTION

A fundamental understanding of the dynamics of the formation, deformation, and coalescence of charged droplets in an electric field is important to various applications, including electro-spray ionization,[1] ink-jet printing,[2] electro-wetting,[3,4] manipulation of droplets,[5,6] high-throughput injection,[7] and de-emulsification.[8–10] In the absence of external fields, two neutral droplets without stabilizers spontaneously coalesce upon contact, thereby minimizing the total surface energy.[11] Such coalescence is suppressed when direct contact of the droplet interfaces is prevented by stabilizers such as surfactants or colloidal particles. In an electric field, droplets experience an electric stress that can stretch them, as well as surface tension that drives them towards adopting a spherical shape. The shape-deformation dynamics is thus governed by the interplay between these two stresses. Two oppositely charged droplets attract, and as a result, approach each other in an electric field. When the electric stress exceeds the surface tension stress, these two adjacent droplets are stretched until they touch and coalesce.[9,12,13] In fact, a strong electric field can also cause neighboring particle-stabilized emulsion drops to form transient bridges, which can eventually grow to cause coalescence of the drops.[10] However, contrary to the common perception that droplets of opposite charge should always attract and coalesce, two such droplets can coalesce only partially or recoil from each other upon contact, even if the electric field is strong.[12,14–18] While it is evident that the presence of an electric field enriches the dynamic behavior of emulsion droplets, the interplay between electric and surface tension stresses still remains inadequately understood.

a)Author to whom correspondence should be addressed. Electronic mail: ashum@hku.hk.

In this work, we use a simple model geometry to systematically study the dynamics of oppositely charged droplets. We place a pair of emulsion droplets with different separation distances in an electric field and investigate the resulting dynamic behaviors. We find that in a strong electric field, the electric stress always forces the two droplets to contact and discharge; however, upon such contact, depending on the initial distance between the droplets, three distinctly different dynamic regimes of subsequent droplet behavior emerge. Besides a simple "coalescence" regime, which is similar to that of neutral droplets, we find two additional dynamic regimes, which we refer to as "fuse-and-split" and "periodic non-coalescence." These novel dynamical behaviors, which cannot be observed among uncharged droplets, can be accounted for by the geometry of the droplets that results from the electric field, and the separation distance before the droplets touch. We demonstrate that, despite the electrical charging, droplets get instantly discharged upon contact. Immediately afterwards, a short bridge forms between the droplets, and surface tension determines the subsequent dynamics. Our work illustrates the intricate interplay between surface tension and electric forces in the dynamics of droplets and extends our understanding of their deformation and coalescence behavior, which is of great interest to the fate of electrified drops in fields including cloud physics and electrohydrodynamics. Similar experiments could serve as a tool for characterizing the efficiency of surfactants or colloidal particles in preventing droplet coalescence.

II. EXPERIMENTAL

We investigate the behavior of a pair of water droplets pinned to needles and submerged in a continuous oil phase within a custom-built poly (methyl methacrylate) (PMMA) container, as shown schematically in Fig. 1(a). We use 0.01M potassium chloride (KCl) aqueous solution as the dispersed phase, which has an electrical conductivity of 1.2×10^{-3} S/cm. Liquid paraffin (density: 0.84 kg/l, viscosity: 36 mPa·s, dielectric constant: 2.2; Aladdin Reagent, China) is used as the continuous phase; the interfacial tension γ between the oil and water is 40 mN/m (Tensiometer, Kruss-SITE100). Two round metallic needles (outer diameter: 0.9 mm) are inserted and aligned from opposite sides of the container with a separation distance L. Two droplets are injected using syringe pumps (Longer pumps, China) at a low flow rate of 50 μl/h into the container through the needles; the surface-to-surface distance between the two droplets is defined as h. The resultant droplets remain attached to the nozzles. When the drops reach the desired radii, R_1 and R_2, we stop the injection and let the droplets sit until the size of the spherical drops remains stable for a few minutes. The droplets have a diameter ranging from 0.7 mm to 1.3 mm. At the beginning of the experiment, both droplets have similar size: $R_1/R_2 = 1.0 \pm 0.1$. During the experiment, the size ratio of the two droplets can change to a maximum value of $3 < R_1/R_2 < 5$, where R_1 denotes the radius of the larger droplet. We define a relative separation h/R, where $R = ((R_1^3 + R_2^3)/2)^{1/3}$ is a

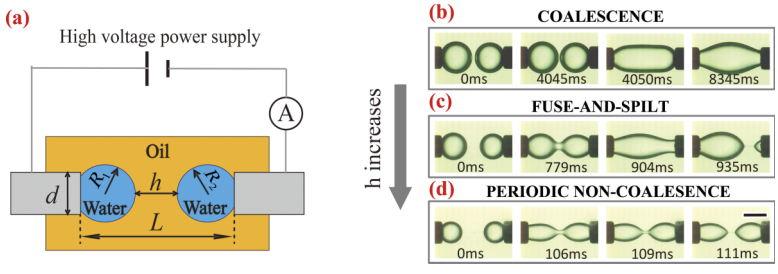

FIG. 1. Dynamics of oppositely charged droplets in an electric field. Schematic experimental setup (a). A pair of water droplets submerged in oil is oppositely charged by a high voltage supply. The corresponding current is monitored by an ammeter (indicated by the letter A in a circle). Images taken with our high-speed camera, showing the dynamics of a pair of droplets under the influence of a strong electric field: Droplets coalesce when h/R is small, $Ca_e = 58$, $h/R = 0.29$, (b). Droplets first fuse into a jet and then split into two droplets at larger relative separations, here $Ca_e = 76$, $h/R = 0.91$, (c). Periodic non-coalescence of droplets happens when the relative separation is sufficiently large, here $Ca_e = 20$, $h/R = 1.92$, (d). The scale bar corresponds to 1 mm.

volume-averaged radius obtained from the initial radii of the individual droplets. The balance between gravitational and capillary forces is determined by the Bond number: $B_o = (\rho_w - \rho_o)R^2 g/\gamma$, where ρ_w and ρ_o are the density of the water and oil, respectively, and g is the acceleration of gravity. Note that in our experiment, the density contrast between the droplets and the ambient fluid is much smaller than that for droplets in air, which leads to a small Bond number: $B_0 \ll 1$. Therefore, the effect of gravity can be neglected. To start our dynamic experiments, we apply a voltage U to the droplets using a high voltage power supply (power: 100 W, rated current: 3 mA; Tianjian Dongwen, China) and monitor the evolution of the current using an ammeter (660E, CH Instrument, TX, USA), as also shown in Fig. 1(a). The corresponding droplet dynamics are recorded using a high-speed camera (Phantom v9.1, Vision Research, Inc., Wayne, NJ, USA).

III. RESULTS AND DISCUSSION

The electric stress, which scales with the applied electric field as $\varepsilon_0\varepsilon_d E_0^2$, competes with the Laplace pressure, which scales as γ/R, and causes the droplets to stretch and adopt an elliptical shape.[19–21] The ratio of these two stresses can be expressed as a dimensionless electrocapillary number $Ca_e = \varepsilon_0\varepsilon_d E_0^2 R/\gamma$, with ε_d the dielectric constant of the outer liquid, ε_0 the vacuum permittivity, $E_0 = U/h$ the electric field strength between the droplets, and γ the surface tension. At small enough Ca_e, two neighboring droplets wit $h/R > 0$ remain separated (Fig. 2, filled circles/green) as the electric stress cannot overcome the surface tension stress and stretch the droplets to bring them into contact [see also the multimedia movie in Fig. 2 (Multimedia view)]. Our experiments indicate that the critical electrocapillary number below which drops remain separated is nearly independent of the relative separation h/R and of order 1, as shown in Fig. 2. These results agree with previous studies on the contact of two free droplets driven by an electric stress[12,13] (see the supplementary material[22] for the comparison of the results).

When Ca_e is above this critical value, the electric stress overcomes the surface tension stress and the droplets stretch until they eventually touch. We observe that subsequent to such contact, droplets exhibit three different types of dynamic behaviors: "coalescence," "fuse-and-split," and "periodic non-coalescence." At small h/R, drops are only slightly stretched when they come in

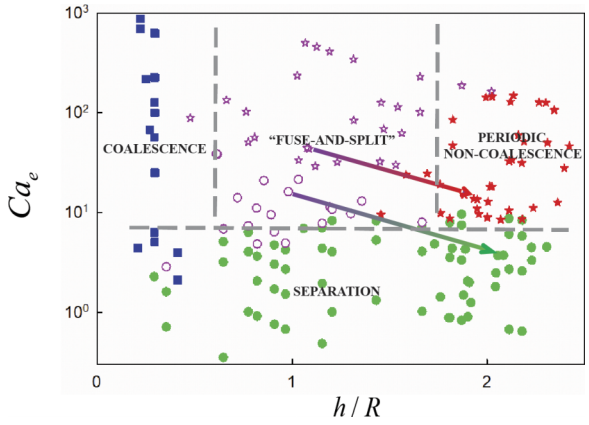

FIG. 2. State diagram for the dynamic behaviors of droplet pairs, based on the electrocapillary number $Ca_e = \varepsilon_0\varepsilon_d E_0^2 R/\gamma$, and the relative separation h/R. The phase map contains 160 independent measurements and is highly reproducible. Four regimes are identified: (1) separation: two droplets remain separated, as denoted by filled circles/green; (2) coalescence: two droplets coalesce into a single jet, as denoted by filled squares/blue; (3) "fuse-and-split": two droplets first fuse into a jet and then split into droplets again, as denoted by open stars/purple and open circles/purple. This is a transition state; after one or several "fuse-and-split" events, droplets eventually move towards either the periodic non-coalescence or the separation regime, depending on the value of the electrocapillary number; the transitions are indicated by the arrows with gradient colors; (4) periodic non-coalescence: two droplets go through cycles of periodic non-coalescence indefinitely, as denoted by filled stars/red. (Multimedia view) [URL: http://dx.doi.org/10.1063/1.4928854.1] [URL: http://dx.doi.org/10.1063/1.4928854.2] [URL: http://dx.doi.org/10.1063/1.4928854.3] [URL: http://dx.doi.org/10.1063/1.4928854.4] [URL: http://dx.doi.org/10.1063/1.4928854.5] [URL: http://dx.doi.org/10.1063/1.4928854.6]

contact with each other and they subsequently coalesce to form a stable jet, as shown in Fig. 1(b) [see also multimedia movie in Fig. 2 (Multimedia view)]; break-up does not happen since the length of the jet is smaller than the perimeter of its circular cross section.[23] We refer to this regime as the "coalescence" regime (Fig. 2, filled squares/blue); this regime is also expected to occur for two neutral droplets that are brought in contact with each other.

At larger values of h/R, droplets with high enough Ca_e first coalesce into a jet similar to that formed in the "coalescence" regime; however, here the jet is unstable and subsequently breaks up into two droplets again, as shown in Fig. 1(c) [see also multimedia movie in Fig. 2 (Multimedia view)]. We term this new dynamic behavior "fuse-and-split," plotted as open stars and open circles/purple in the state diagram in Fig. 2.

At the largest values of h/R, we observe the formation of conical tips in both droplets near the point of contact. Subsequently, even though a brief contact occurs, the droplets do not coalesce; instead, they bounce away from each other rapidly, as shown in Fig. 1(d) [see also multimedia movie in Fig. 2 (Multimedia view)]. The separated droplets subsequently repeat this cycle of approach and rebound indefinitely, until the voltage is turned off. We therefore refer to this regime as the "periodic non-coalescence" regime, indicated by filled stars/red in the state diagram in Fig. 2.

The dynamic behaviors of the charged droplets are also reflected in the time-dependence of the electrical current. When the droplets are separated, the current is zero. However, the current rises dramatically upon contact, after which it decreases and subsequently evolves according to the respective dynamic regime. Spikes in electrical current coincide with the moment of droplet contact, as can be seen by comparing the insets with the corresponding data in Fig. 3; we interpret these spikes as corresponding to a rapid discharging process that occurs right after the initial droplet contact. After this initial spike, in both the "coalescence" and the "fuse-and-split" regimes, we observe a continuous increase of the current as a function of time, which in both cases coincides with the formation of a liquid bridge that causes a decrease in the electrical resistance between the injection needles. The increase is more pronounced in the "coalescence" regime than in the "fuse-and-split" regime, consistent with the larger cross-sectional area of the bridge in the first case compared to the second case. Additionally, in the "fuse-and-split" regime, the current again drops to zero after break-up of the bridge. In contrast, for the "periodic non-coalescence" regime, the current decreases to zero immediately following the spike and does not grow subsequently, in agreement with the observed full separation of the droplets immediately after droplet contact. In this case, the process repeats itself indefinitely, as shown in Fig. 3(c) for two consecutive non-coalescence events.

The observed rapid discharging of the droplets reduces the electric stress. Before contact, the droplets are oppositely charged and have a typical surface charge density of $\varepsilon_0\varepsilon_d E_0$. Upon droplet contact, the droplets discharge. This happens in a characteristic time scale $\tau_r = \varepsilon_0\varepsilon_d/\sigma_d$,[24,25] where σ_d is the conductivity of the droplet phase. Therefore, the magnitude of the current spikes caused by

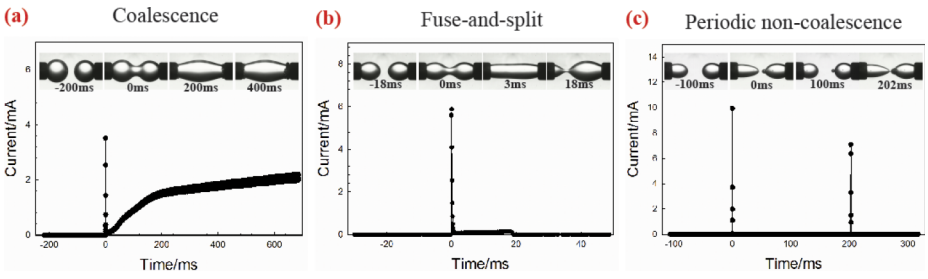

FIG. 3. Measured electrical current as a function of time in the three different dynamic regimes, with corresponding images of the charged droplets. In all three cases ((a)-(c)), the current increases sharply upon initial droplet contact; the resultant current spike exceeds the value of current threshold (3 mA) for overcurrent protection. (a) Coalescence regime: following the current spike, the current increases continuously, reflecting the formation of a stable liquid bridge. (b) "Fuse-and-split" regime: after the spike, the current rises as the droplets coalesce into a jet. It drops to zero when the jet splits (see inset image at 18 ms); (c) "periodic non-coalescence" regime: current spikes occur periodically as the droplets contact repeatedly. The applied voltage for the experiments is 2 kV. The time resolution for all the current plots is $8 \cdot 10^{-5}$ s. The outer diameter of the nozzle in the optical images is 0.9 mm.

the discharging of the droplets is on the order of $\sigma_d E$. In our experiments, the electrical conductivity is relatively large ($\sigma_d \approx 1.2 \times 10^{-3}$ S/cm); as a result, the current spikes can exceed the threshold current (3 mA) allowed by the instrument for safety reasons (Fig. 3). This causes the current to decrease to zero after the observed spikes. To further confirm that the rapid discharging indeed causes the rise in current upon droplet contact and then subsequently leads to the decrease of the current, we have carried out experiments using deionized water droplets with a much lower electric conductivity ($\sigma_d \approx 5.5 \times 10^{-6}$ S/cm) than the salty water (see the supplementary material[22]). We indeed observe that also in this case, the current rapidly rises right upon droplet contact (see Fig. S1 in the supplementary materials[22]). In this case, however, the values of the current right after this rise are on the order of 10^{-5} A, and thus much smaller than the values measured with salty water, which are on the order of 10^{-3} A; note that the observed decrease is comparable to the corresponding decrease in conductivity. Considering this current is smaller than the threshold value (3 mA), it does not subsequently decrease to zero, but rather maintains a relatively constant value presumably determined by the applied voltage and the electrical resistance of the bridge. Our results are thus supportive of our interpretation that the rise in electrical current results from rapid discharging of the salty droplets which can subsequently cause the decrease of current.

Immediately after the initial droplet contact, as soon as the droplets discharge, surface tension starts to dominate the dynamics of the droplets. In our experiments, the typical time scale for the discharging process is $\tau_r = 5.8 \cdot 10^{-10}$ s. To identify the relevant time scale in the coalescence process, we estimate the Ohnesorge number $Oh = \tau_v/\tau_c$, where $\tau_v = \mu R/\gamma$ and $\tau_c = \sqrt{\rho R^3/\gamma}$, with ρ and μ the density and viscosity of the fluid, are the viscous-capillary and inertial-capillary time scales. Since in our experiments, $Oh << 1$, viscous effects are negligible and the characteristic time scale of coalescence is τ_c. Furthermore, we find that $\tau_c \approx 6$ ms, which is around seven orders of magnitude larger than the time scale for the discharging process. As a result, the droplets are essentially discharged instantaneously upon contact and surface tension immediately dominates the subsequent dynamic behavior of the droplets.

Normally, two uncharged droplets would always coalesce upon contact driven by surface tension. However, our experiments show that droplets can separate from each other immediately after the initial contact, with the subsequent dynamic behaviors depending critically on the initial separation distance between the droplets. Interestingly, recent models and computer simulations propose to interpret non-coalescence phenomena in terms of the shape of the bridge that forms between the droplets right after contact.[16,26,27] Based on this, we hypothesize that the rich dynamics observed for our charged droplets can be accounted for by the different geometric conditions set by the imposed electric stress and separation distance before droplet contact. When two droplets touch, a short liquid bridge forms between them. Whether the droplets coalesce or not is then determined by the pressure difference between the bridge, P_{bridge}, and the droplets, P_{bulk}, which can be estimated using the Young-Laplace equation as[15]

$$\Delta P = P_{bridge} - P_{bulk} = \gamma \cdot (1/R_s - 1/R_a) - 2\gamma/R_{bulk}, \quad (1)$$

where R_s and R_a are the principal radii of curvature of the liquid bridge, with R_s corresponding to the radius of the smallest cross section of the bridge, as indicated in the inset in Fig. 4(a), and R_{bulk} is the radius of the droplets. Considering that $R_{bulk} >> R_s$, R_a, the second term in the previous equation can be neglected. As a result, $\Delta P \approx \gamma \cdot (1/R_s - 1/R_a)$. Hence, depending on whether $R_s > R_a$ or $R_s < R_a$, the bridge either grows or thins, respectively. The competition between these two effects can be characterized by the intersection angle between the slopes of the of droplets' surfaces right at contact, as indicated in the inset in Fig. 4(a). This angle is then given by $\tan(\theta/2) = R_a/R_s$.[15] When $\theta < 90°$, $1/R_a$ is the dominating curvature and $\Delta P < 0$, resulting in coalescence. By contrast, when $\theta > 90°$, $1/R_s$ is the dominating curvature and $\Delta P > 0$, resulting in non-coalescence. In our experiment, the intersection angle θ can be precisely controlled by setting the relative separation of the droplets. When the relative separation h/R is small, droplets are slightly stretched and form a small angle θ upon contact, thus causing coalescence (Fig. 4(a), filled dots). This is similar to the coalescence behavior exhibited by neutral droplets. At large h/R, droplets become highly stretched and θ is large; as a consequence, non-coalescence is observed (Fig. 4(a), open dots). At the critical

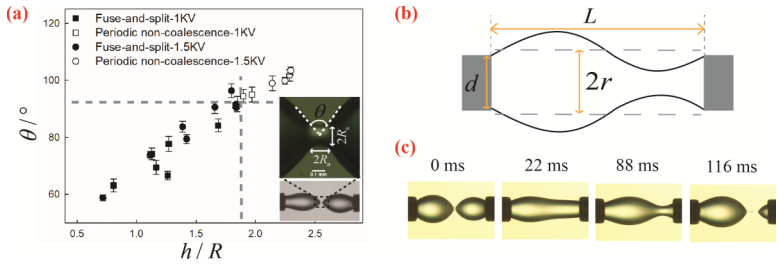

FIG. 4. (a) A plot of the intersection angle θ formed between two contacting droplets (insets) versus relative separation h/R, as shown by the insets. Small h/R leads to small θ, where droplets coalesce following contact as indicated by the filled squares (voltage: 1 kV) and filled circles (voltage: 1.5 kV); by contrast, large h/R leads to large θ, where non-coalescence occurs as shown by the open squares (voltage: 1 kV) and open circles (voltage: 1.5 kV); the dashed lines represent the boundaries between the coalescence and non-coalescence. (b) Schematic of the corrugated jet pinned between two nozzles. The dashed lines depict the corresponding unperturbed jet of equal volume, with radius r. The jet is unstable when $L > 2\pi r$. (c) Evolution of the coalesced jet in the regime of "fuse-and-split." The coalesced jet following the droplets contact will evolve into a single wave corrugation and lead to the splitting of the jet into two droplets with different sizes.

relative separation $h/R \approx 1.8$ which characterizes the transition between "fuse-and-split" and "periodic non-coalescence" on the state diagram in Fig. 2, droplets intersect at an angle of approximately 90°, consistent with the critical angle predicted from the above theoretical arguments. We notice that this critical h/R is slightly larger than that for two free droplets in an electric field, as studied by Thiam *et al.*[12] We attribute this difference to the different geometry in these experiments: Droplets are pinned at the nozzles in our experiment while they are free in the experiments of Thiam *et al.*[12] (see the supplementary material[22] for the comparison of the results).

When the relative initial separation h/R is smaller than a critical value of 1.8, droplets coalesce and form a jet. The subsequent fate of this jet depends on the exact value of the relative separation. The jet will remain stable for small h/R, which represents the regime of "coalescence"; it splits into two droplets of different size at larger h/R, which represents the regime of "fuse-and-split." As surface tension dominates the dynamics after coalescence, we analyze the fate of the pinned jet using linear stability analysis. In this context, the pinned jet is unstable when its length exceeds the length of its circumference.[28] In our experiments, the jet radius is determined by the initial relative separation h/R of the droplets, according to mass conservation. Hence, a larger h/R leads to a smaller jet radius. Thus, there exists a critical value of h/R where the jet radius satisfies the splitting condition, $2\pi r = L$, where L and r are the length and the radius of the jet, respectively. This analysis yields a critical value of $h/R \approx 1$ (see the supplementary material[22] for the calculation of the critical h/R), which is close to the value $h/R \approx 0.5$ where a transition between the "coalescence" and the "fuse-and-split" regimes is observed experimentally (Fig. 2). In addition, since we only fit one wavelength in the length L, and there are no restrictions for the fluid at the bounding needles, the amplitude maximum and minimum can occur anywhere within L (see Fig. 4(b)). As a result, jet break-up will generally result in droplets of different sizes, as we also observe experimentally (see Fig. 4(c)).

We also note that the "fuse-and-split" is an unstable regime that does not occur indefinitely. After each "fuse-and-split" step, the increasing size difference between the droplets always leads to larger h/R and smaller Ca_e. As a consequence, eventually the two resultant droplets cannot overcome this increased separation and remain separated indefinitely [see multimedia movie in Fig. 2 (Multimedia view)], as shown by the open circles in the phase diagram (Fig. 2). We confirm this by directly calculating the change in h/R and Ca_e during "fuse-and-split" events. For an event with initial $h/R = 0.98$ and $Ca_e = 16$, the resultant droplets after the first "fuse-and-split" event have $h/R = 2.05$ and $Ca_e = 3.7$, as shown by the arrow with a color gradient in the phase diagram; the system thus enters the regime where the field is unable to pull the drops together. Alternatively, at higher electric field strengths, the droplet dynamics can transition from the "fuse-and-split" regime to the "periodic non-coalescence" regime (see multimedia movie in Fig. 2 (Multimedia view)), as shown by the open stars in the phase diagram. In a representative event with initial $h/R = 1.09$ and $Ca_e = 43.6$, after the first "fuse-and-split" event, we have $h/R = 1.95$ and $Ca_e = 12.7$, as indicated

by the arrow with gradient color in the phase diagram; the resultant droplets now lie in the "periodic non-coalescence" regime, where droplet approach and separation repeat indefinitely.

IV. CONCLUSION

We have investigated the dynamic behavior of oppositely charged droplets pinned to needles. Our work demonstrates that the interplay of electrostatics and surface tension leads to rich dynamics, which we rationalize by constructing a state diagram expressed as a function of the electrocapillary number and the relative separation between the droplets. Apart from the common "coalescence," similar to the classic picture of neutral droplet coalescence, we have found two new and previously unreported dynamic regimes: "fuse-and-split" and "periodic non-coalescence." Our investigation further indicates that upon initial contact, droplets are rapidly discharged and, as a consequence, surface tension rather than the electric stress dominates the subsequent dynamics. By analyzing the corresponding capillary instability, all the observed dynamical regimes can be attributed to the different shapes of the droplets at the time of contact; this shape is determined by the relative separation h/R of the droplets. We further demonstrate that droplets in the unstable "fuse-and-split" regime eventually transition into a different dynamic regime; they either become stably separated or enter the "periodic non-coalescence" regime as a result of the increased h/R and decreased Ca_e after the splitting event. Our work enhances the understanding of the dynamics of electrically charged droplets and the observed behaviors should be generally applicable to emulsions stabilized by both surfactants and particles. We expect that the critical values of electrocapillary numbers and relative separation depend critically on emulsion stability. Thus, our work could also inspire the development of new methods for measuring emulsion stability or the performance of stabilizers.

ACKNOWLEDGMENTS

We would like to thank Dr. Robert C. Roberts for help with measuring electric current. This research was supported by the Early Career Scheme (No. HKU 707712P), the General Research Fund (Nos. HKU 719813E and 17304514), the NWO/RGC Joint Research Scheme sponsored by the Research Grants Council of Hong Kong and the Netherlands Organization for Scientific Research (No. D-HK009/11T), the Young Scholar's Program (No. NSFC51206138/E0605) from the National Natural Science Foundation of China as well as the Seed Funding Program for Basic Research (No. 201101159009), and Small Project Funding (No. 201109176165) from the University of Hong Kong. A.F.N. is supported by the NSF (No. CBET-0967293).

[1] J. B. Fenn, M. Mann, C. K. Meng, S. F. Wong, and C. M. Whitehouse, "Electrospray ionization for mass spectrometry of large biomolecules," Science (New York, N.Y.) **246**, 64 (1989).
[2] P. Calvert, "Inkjet printing for materials and devices," Chem. Mater. **13**, 3299 (2001).
[3] M. G. Pollack, A. D. Shenderov, and R. B. Fair, "Electrowetting-based actuation of droplets for integrated microfluidics," Lab Chip **2**, 96 (2002).
[4] J.-C. Baret and F. Mügele, "Electrical discharge in capillary breakup: Controlling the charge of a droplet," Phys. Rev. Lett. **96**, 016106 (2006).
[5] M. Abdelgawad and A. R. Wheeler, "The digital revolution: A new paradigm for microfluidics," Adv. Mater. **21**, 920 (2009).
[6] D. R. Link, E. Grasland-Mongrain, A. Duri, F. Sarrazin, Z. Cheng, G. Cristobal, M. Marquez, and D. A. Weitz, "Electric control of droplets in microfluidic devices," Angew. Chem., Int. Ed. **45**, 2556 (2006).
[7] A. R. Abate, T. Hung, P. Mary, J. J. Agresti, and D. A. Weitz, "High-throughput injection with microfluidics using picoinjectors," Proc. Natl. Acad. Sci. U. S. A. **107**, 19163 (2010).
[8] X. Niu, F. Gielen, A. J. deMello, and J. B. Edel, "Electro-coalescence of digitally controlled droplets," Anal. Chem. **81**, 7321 (2009).
[9] J. S. Eow, M. Ghadiri, A. O. Sharif, and T. J. Williams, "Electrostatic enhancement of coalescence of water droplets in oil: A review of the current understanding," Chem. Eng. J. **84**, 173 (2001).
[10] G. Chen, P. Tan, S. Chen, J. Huang, W. Wen, and L. Xu, "Coalescence of pickering emulsion droplets induced by an electric field," Phys. Rev. Lett. **110**, 064502 (2013).
[11] P. G. de Gennes, F. Brochard-Wyart, D. Quéré, and A. Reisinger, *Capillarity and Wetting Phenomena: Drops, Bubbles, Pearls, Waves* (Springer, New York, 2004).
[12] A. R. Thiam, N. Bremond, and J. Bibette, "Breaking of an emulsion under an ac electric field," Phys. Rev. Lett. **102**, 188304 (2009).

[13] P. R. Brazier-Smith, S. G. Jennings, and J. Latham, "An investigation of the behaviour of drops and drop-pairs subjected to strong electrical forces," Proc. R. Soc. London, Ser. A **325**, 363 (1971).
[14] H. T. Ochs and R. R. Czys, "Charge effects on the coalescence of water drops in free fall," Nature **327**, 606 (1987).
[15] W. D. Ristenpart, J. C. Bird, A. Belmonte, F. Dollar, and H. A. Stone, "Non-coalescence of oppositely charged drops," Nature **461**, 377 (2009).
[16] J. C. Bird, W. D. Ristenpart, A. Belmonte, and H. A. Stone, "Critical angle for electrically driven coalescence of two conical droplets," Phys. Rev. Lett. **103**, 164502 (2009).
[17] B. S. Hamlin, J. C. Creasey, and W. D. Ristenpart, "Electrically tunable partial coalescence of oppositely charged drops," Phys. Rev. Lett. **109**, 094501 (2012).
[18] J. Wang, B. Wang, and H. Qiu, "Coalescence and breakup of oppositely charged droplets," Sci. Rep. **4**, 7123 (2014).
[19] G. Taylor, "Disintegration of water drops in an electric field," Proc. R. Soc. London, Ser. A **280**, 383 (1964).
[20] Q. Wang, Z. Suo, and X. Zhao, "Bursting drops in solid dielectrics caused by high voltages," Nat. Commun. **3**, 1157 (2012).
[21] R. T. Collins, K. Sambath, M. T. Harris, and O. A. Basaran, "Universal scaling laws for the disintegration of electrified drops," Proc. Natl. Acad. Sci. U. S. A. **110**, 4905 (2013).
[22] See supplementary material at http://dx.doi.org/10.1063/1.4928854 for (a) discharging current of water droplets with a lower electric conductivity; (b) calculation of the critical h/R separating stable and unstable bridges; (c) comparison between our results and the results in previous studies.
[23] Beer, "Über die Oberflächen rotierender Flüssigkeiten im Allgemeinen, insbesondere über den Plateau'schen rotationsversuch," Ann. Phys. Chem. **172**, 1 (1855).
[24] J. R. Melcher and G. I. Taylor, "Electrohydrodynamics: A review of the role of interfacial shear stresses," Annu. Rev. Fluid Mech. **1**, 111 (1969).
[25] D. A. Saville, "Electrohydrodynamics: The Taylor-Melcher leaky dielectric model," Annu. Rev. Fluid Mech. **25**, 27 (1997).
[26] H. Sebastian and T. Peter, "Bouncing of charged droplets: An explanation using mean curvature flow," Europhys. Lett. **104**, 34001 (2013).
[27] C. T. Bartlett, G. A. Généro, and J. C. Bird, "Coalescence and break-up of nearly inviscid conical droplets," J. Fluid Mech. **763**, 369 (2015).
[28] J. Eggers and E. Villermaux, "Physics of liquid jets," Rep. Prog. Phys. **71**, 036601 (2008).